

Available online at [www.sciencedirect.com](http://www.sciencedirect.com)

ScienceDirect

journal homepage: [www.jfda-online.com](http://www.jfda-online.com)

## Original Article

# Analysis of titanium dioxide and zinc oxide nanoparticles in cosmetics



Pei-Jia Lu<sup>\*</sup>, Shou-Chieh Huang, Yu-Pen Chen, Lih-Ching Chiueh,  
Daniel Yang-Chih Shih

Food and Drug Administration, Ministry of Health and Welfare, Taipei, Taiwan

## ARTICLE INFO

## Article history:

Received 11 April 2014

Received in revised form

21 October 2014

Accepted 25 February 2015

Available online 20 April 2015

## Keywords:

nanoparticles

sunscreens

titanium dioxide

zinc oxide

## ABSTRACT

There have been rapid increases in consumer products containing nanomaterials, raising concerns over the impact of nanoparticles (NPs) to humankind and the environment, but little information has been published about mineral filters in commercial sunscreens. It is urgent to develop methods to characterize the nanomaterials in products. Titanium dioxide (TiO<sub>2</sub>) and zinc oxide (ZnO) NPs in unmodified commercial sunscreens were characterized by laser scanning confocal microscopy, atomic force microscopy, X-ray diffraction (XRD), and transmission electron microscopy (TEM). The results showed that laser scanning confocal microscopy evaluated primary particle aggregates and dispersions but could not size NPs because of the diffraction limited resolution of optical microscopy (200 nm). Atomic force microscopy measurements required a pretreatment of the sunscreens or further calibration in phase analysis, but could not provide their elemental composition of commercial sunscreens. While XRD gave particle size and crystal information without a pretreatment of sunscreen, TEM analysis required dilution and dispersion of the commercial sunscreens before imaging. When coupled with energy-dispersive X-ray spectroscopy, TEM afforded particle size information and compositional analysis. XRD characterization of six commercial sunscreens labeled as *nanoparticles* revealed that three samples contained TiO<sub>2</sub> NPs, among which two listed ZnO and TiO<sub>2</sub>, and displayed average particle sizes of 15 nm, 21 nm, and 78 nm. However, no nanosized ZnO particles were found in any of the samples by XRD. In general, TEM can resolve nanomaterials that exhibit one or more dimensions between 1 nm and 100 nm, allowing the identification of ZnO and TiO<sub>2</sub> NPs in all six sunscreens and ZnO/TiO<sub>2</sub> mixtures in two of the samples. Overall, the combination of XRD and TEM was suitable for analyzing ZnO and TiO<sub>2</sub> NPs in commercial sunscreens.

Copyright © 2015, Food and Drug Administration, Taiwan. Published by Elsevier Taiwan

LLC. Open access under [CC BY-NC-ND license](https://creativecommons.org/licenses/by-nc-nd/4.0/).

<sup>\*</sup> Corresponding author. Food and Drug Administration, Ministry of Health and Welfare, No. 161-2, Kunyang Street, Nangang District, Taipei City 115-61, Taiwan.

E-mail address: [andreaander@fda.gov.tw](mailto:andreaander@fda.gov.tw) (P.-J. Lu).

<http://dx.doi.org/10.1016/j.jfda.2015.02.009>

1021-9498/Copyright © 2015, Food and Drug Administration, Taiwan. Published by Elsevier Taiwan LLC. Open access under [CC BY-NC-ND license](https://creativecommons.org/licenses/by-nc-nd/4.0/).

## 1. Introduction

The rapid development of nanotechnology has resulted in an increasing number of nanomaterial-based consumer products and industries. Because of their unique physical properties, nanomaterials have dramatically transformed the function and application of commercial products, including wound dressings, cosmetics, detergents, food packaging, drug delivery, biosensors, and antimicrobial coatings [1]. Recently, titanium dioxide (TiO<sub>2</sub>) and zinc oxide (ZnO) nanoparticles (NPs) have gained popularity as inorganic physical sunscreens because they can reflect and scatter UVA and UVB radiations while preventing skin irritation and disruption of the endocrine system typically induced by chemical UV filters. Also, these NPs may be transparent and pleasant to touch [1,2]. However, safety concerns regarding their utilization in consumer products have recently emerged. Reports have suggested that sunscreen NPs induce cyto- and genotoxicity through oxidative stress [3]. Zvyagin et al [4] and Tilman et al [5] have shown that TiO<sub>2</sub> and ZnO NPs could not penetrate the deep layers of healthy adult skin. In contrast, Wu et al [6] demonstrated that TiO<sub>2</sub> NPs could enter the deep layers of porcine epidermis as well as hairless mouse skin. Because the impact of NPs on humans is poorly understood, no clear regulation has been implemented for NPs among international authorities.

The International Cooperation on Cosmetic Regulation define a nanomaterial in cosmetics as an insoluble, intentionally manufactured ingredient with one or more dimensions ranging from 1 nm to 100 nm in the final formulation. In addition, the nanomaterial must be sufficiently stable and persistent in biological media to enable potential interactions with biosystems [7]. In 2012, the International Organization for Standardization underlined that the physicochemical characterization of nanomaterials was critical for the identification of test materials before toxicological assessment (ISO/TR13014). Physicochemical parameters include particle size/particle size distribution, aggregation/agglomeration state, shape, surface area, composition, surface chemistry, surface charge, and solubility/dispersibility [8]. A safety guideline on nanomaterials in cosmetics issued by the United States Food and Drug Administration [9] recommended that the product be evaluated by analyzing these physicochemical properties. NPs may aggregate when added to cosmetics, making their characteristics in the final products essential.

Sunscreen formulations are very complex and opaque, hindering NP detection and characterization. Finding appropriate analytical methods to achieve this characterization without product modification and misleading dilution is an important issue. Some studies have investigated single particles in noncomplex matrices [10,11] but few reports have discussed NP characteristics in complex formulations. Tyner et al [12] have evaluated the ability of 20 analytical methods to detect TiO<sub>2</sub> and ZnO NPs in unmodified commercial sunscreens. Variable-pressure scanning electron microscopy, atomic force microscopy (AFM), laser scanning confocal microscopy (LSCM), and X-ray diffraction (XRD) were considered applicable and complementary for NP characterization in

sunscreens. Guidelines on the safety assessment of nanomaterials in cosmetics from the Scientific Committee on Consumer Safety suggested the use of at least two methods, of which one should be electron microscopy, preferably high-resolution transmission electron microscopy (TEM), to determine size nanomaterial parameters [13]. Here the size parameters of NPs in six different commercial sunscreens were evaluated by TEM, AFM, LSCM, and XRD. Analytical results were compared to assess the effectiveness of these methods in characterizing NP-based cosmetics.

## 2. Materials and methods

### 2.1. Sunscreen samples and NP controls

Six commercial sunscreens were selected based on product descriptions and promotion flyers mentioning the presence of inorganic NPs in their formulation. Table 1 lists inorganic ingredients and their amounts in the cosmetics. Among these sunscreens, two contained only TiO<sub>2</sub>, two contained only ZnO, and two contained a combination of TiO<sub>2</sub> and ZnO. All sunscreens were obtained without prescription; one product was made in Korea, one in France, and the others were produced in the USA. Standard solutions of TiO<sub>2</sub> (107 nm) and ZnO NPs (76 nm) used as control samples were purchased from Sigma–Aldrich (St Louis, MO, USA). The TiO<sub>2</sub> NP standard solution consisted of anatase and rutile crystals.

### 2.2. AFM

AFM analyses were performed using an Asylum Research MFP-3D system (Goleta, CA, USA) in tapping mode. Maximum scan areas were 90 μm × 90 μm. The cantilever and samples were located using a charge-couple device monitor. Unmodified sunscreens were transferred onto a glass slide, flattened with a glass coverslip, and air-dried. Size-related sample imaging was conducted at 10 μm, 5 μm, 2 μm, and 1.2 μm scan widths. Acquired phase and height images were analyzed using Asylum Research IGOR PRO-based software.

### 2.3. Laser scanning confocal microscopy

Laser scanning confocal microscopy (LSCM) characterizations were conducted using a Zeiss LSM 710 LSCM (Wetzlar, Germany) equipped with a HeNe laser ( $\lambda_{\text{HeNe}} = 561 \text{ nm}$ ) and a 63× objective (NA1.4). A small amount of sunscreen was placed on

**Table 1 – Inorganic ingredient contents and sun protection factors (SPF) of analyzed sunscreen products.**

| Product No. | Origin | Claimed ingredients (%) |     | SPF |
|-------------|--------|-------------------------|-----|-----|
|             |        | TiO <sub>2</sub>        | ZnO |     |
| COM 1       | USA    | 5                       | 10  | 30+ |
| COM 2       | USA    | 5                       | 10  | 30+ |
| COM 3       | USA    | —                       | 20  | 30+ |
| COM 4       | Korea  | 1.4                     | —   | 35  |
| COM 5       | France | Not listed              | —   | 50+ |
| COM 6       | USA    | —                       | 6.8 | 30+ |

a glass microscope slide and pressed using a glass coverslip to form translucent appearance until there was no visible movement. Images were acquired at five separate locations in each sample and analyzed using the Zeiss LSM Image Browser software.

## 2.4. XRD

XRD patterns were obtained using a PaNalytical Pro X'Pert Pro X-ray diffractometer (Almelo, The Netherlands) with Cu K $\alpha$  irradiation. Untreated sunscreens were directly transferred onto a metal holder and irradiated at  $2\theta$  angles ranging from  $20^\circ$  to  $90^\circ$  with a step size of 0.03 and a scan speed of 0.01–0.08 steps/s. Data were matched for crystal-phase identification and smoothed for background using X'Pert High Score Plot software. NIST standard reference material 1976b was used to construct plots of full widths at half maximum (FWHMs) against  $2\theta$  in order to get instrumental broadening for all angles. FWHMs of reflections were calculated using Origin 8 (OriginLab, Northampton, MA, USA). Instrumental broadening was calculated using Eq 1:

$$\text{FWHM}_{\text{observe}} = \text{FWHM}_{\text{instrument}} + \text{FWHM}_{\text{size+strain}} \quad (1)$$

The reflections including 011 for anatase TiO $_2$ , 110 for rutile TiO $_2$ , and 010 for ZnO were chosen for size analysis. Primary particle sizes were estimated via the Scherrer equation:

$$D = (0.94 \cdot \lambda) / (\text{FWHM}_{\text{size}} \cdot \cos \theta), \quad (2)$$

where  $D$  is the grain size,  $\lambda$  is X-ray wavelength ( $\lambda = 1.54051 \text{ \AA}$ ), and  $\theta$  is the Bragg angle.

## 2.5. TEM

After shaking commercial sunscreens, aliquots of sunscreens (ca. 0.05 g) were taken from the bottle and diluted with ethanol (8 mL). A drop (10  $\mu\text{L}$ ) of the resulting dispersions was deposited onto a carbon-coated copper grid, wicked using filter

paper, and air-dried at room temperature. Particle sizes and shapes were analyzed at acceleration voltage of 200 kV and magnifications of 10,000–20,000 $\times$ . Elemental compositions were determined by energy-dispersive X-ray spectroscopy (EDS).

## 3. Results and discussion

### 3.1. AFM analysis

Three untreated sunscreens (COM 1, COM 3, and COM 6) were examined by AFM. AFM can detect inorganic NPs in the sunscreen matrix and provide morphological information on the metal oxides but requires another analytical technique to compare NP size [12]. The AFM height images of the NPs in sunscreen samples displayed unobvious contours (Fig. 1) because the NPs were embedded in the soft cosmetic formulation, precluding NP size measurement. Therefore, a phase analysis was performed to distinguish different components from the sunscreen matrix. The phase image of COM 1 presented clearer NP features than height images (Fig. 2A). By contrast, the  $5 \mu\text{m} \times 5 \mu\text{m}$  topographic image of the TiO $_2$  NP standard solution showed some aggregates (Fig. 2B). Furthermore, TiO $_2$  NP sizes ranging from 14.4 nm to 27 nm were measured in the standard solution for a  $2 \mu\text{m} \times 2 \mu\text{m}$  scan area. Because of the complexity of cosmetic formulation, sunscreen samples required additional pretreatment and calibration to obtain clear AFM images, and their elemental composition was not analyzed, suggesting that AFM is not suitable for ZnO and TiO $_2$  NP characterization in commercial products.

### 3.2. LSCM analysis

LSCM is a nondestructive method utilized to estimate particle size and distribution in sunscreens but cannot determine

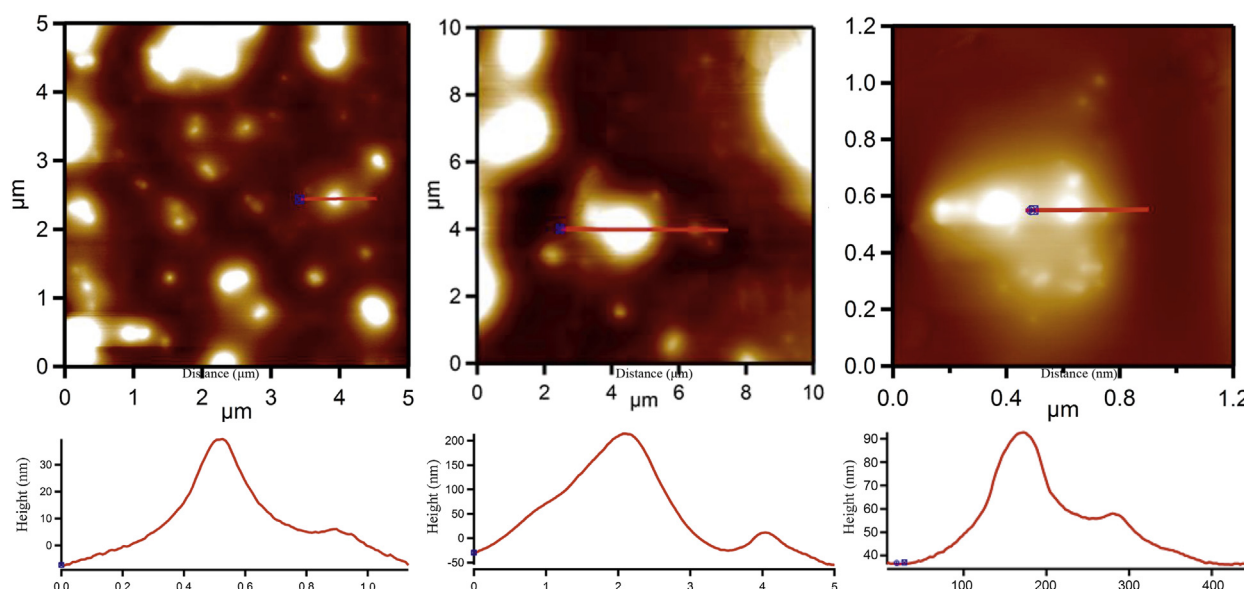
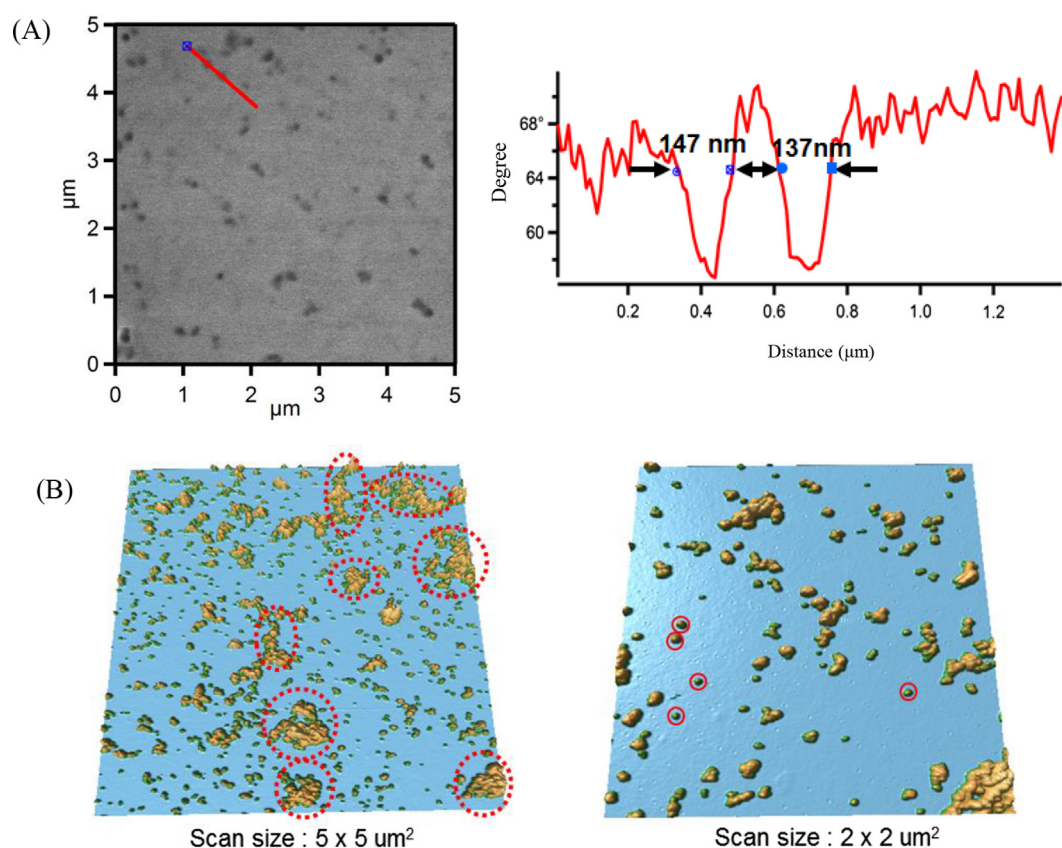


Fig. 1 – Atomic force microscopy height images of commercial sunscreens COM 1, COM 3, and COM 6.



**Fig. 2 – Atomic force microscopy analysis of commercial sunscreens and TiO<sub>2</sub> nanoparticle (NP) standard solution. (A) Phase image of COM 1. (B) Three-dimensional topographical image of the TiO<sub>2</sub> NP standard solution for a scan size of 5 μm × 5 μm (left). Decreasing the scan size (2 μm × 2 μm) enables the morphological determination of TiO<sub>2</sub> NPs (right). The circles highlight the primary particles.**

exact NP sizes [12]. LSCM images of untreated commercial sunscreens COM 1–6 were compared with those of the ZnO NP standard solution (Fig. 3). Sunscreen samples exhibited larger particles than the control solution. In addition, COM 1, COM 2, and COM 5 presented a more even particle dispersion compared with COM 6. LSCM images showed differences in optical contrast between organic residues and inorganic particles present in the sunscreens. LSCM provided insight on the aggregation and dispersion of primary particles but did not differentiate individual NPs because of the limited resolution of optical microscopy (200 nm). In addition, the low contrast of the sunscreen components may limit their resolution because the image contrast was based on different refractive indices [12]. Therefore, LSCM is not appropriate for particle size determination in cosmetic products.

### 3.3. XRD analysis

XRD patterns were acquired to determine crystal properties and grain size in untreated commercial sunscreens. Associated with peak intensities and widths, particle size is generally assumed to induce peak broadening below ca. 200 nm. The larger the FWHM of the peak, the smaller the grain size [12]. The mean grain size of particles within overall samples was estimated using the Scherrer equation (Eq 2) assuming

the absence of strain. XRD reflections of the sunscreen samples are shown in Fig. 4. The reflections including 011 for anatase TiO<sub>2</sub>, 110 for rutile TiO<sub>2</sub>, and 010 for ZnO were chosen for size analysis. The corresponding peaks were at 25.23°, 27.43°, and 31.77°, respectively. COM 4 exhibited weak peak intensities for TiO<sub>2</sub> NPs, consistent with its low TiO<sub>2</sub> content (1.4%). The rutile TiO<sub>2</sub> quantity of COM 4 has been checked at 1.42% by inductively coupled plasma–optical emission spectrometry independently.

By contrast, the other sunscreen samples showed high peak intensities, allowing particle sizes to be calculated. ZnO NPs sizes of 56 nm, 59 nm, 64 nm, and 47 nm were found in COM 1, COM 2, COM 3, and COM 6, respectively. The sharp reflections corresponding to TiO<sub>2</sub> particles provided crystallite sizes below 100 nm in COM 1, COM 2, COM 3, COM 5, and COM 6. TiO<sub>2</sub> NPs can adopt anatase, rutile, or brookite crystalline structures [3]. A stable and abundant pigment, rutile TiO<sub>2</sub>, has commonly been incorporated in sunscreens because of its higher UV absorption and lower photoreactivity compared with anatase [12]. XRD patterns showed that rutile TiO<sub>2</sub> was present in COM 1, COM 2, and COM 4, whereas COM 5 contained a combination of anatase and rutile TiO<sub>2</sub>.

To estimate XRD detection limits, anatase and rutile TiO<sub>2</sub> NP control samples were analyzed at different concentrations, along with ZnO NP control samples (Fig. 5). Anatase TiO<sub>2</sub>



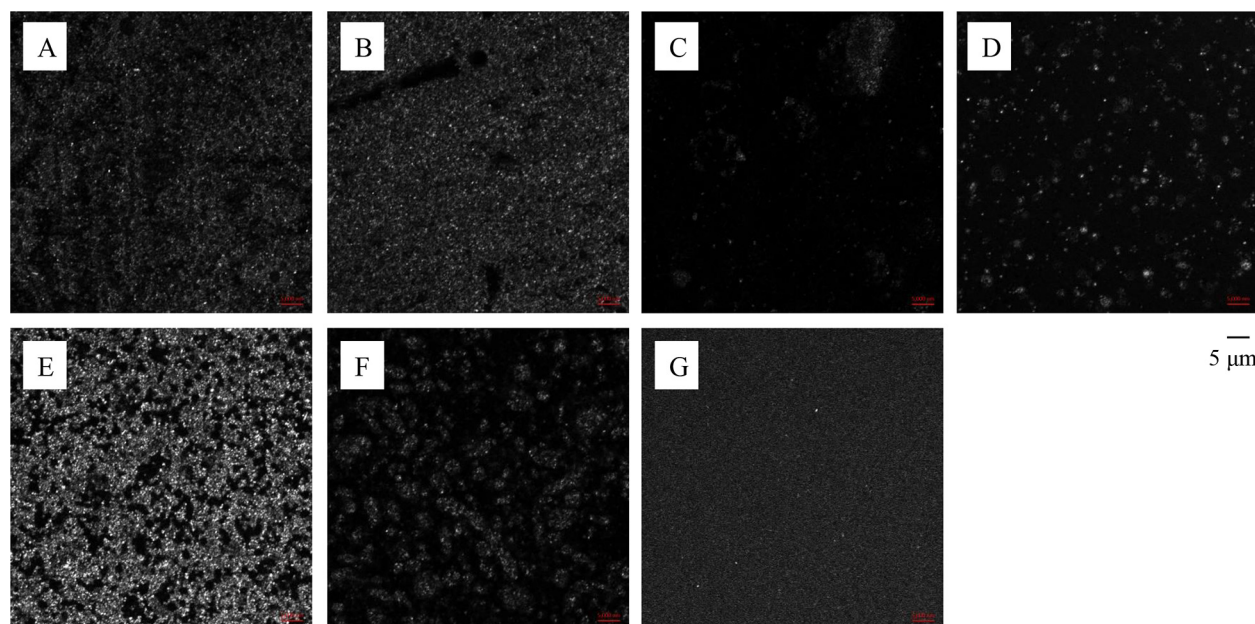


**Fig. 3 – Laser-scanning confocal microscopy of commercial sunscreens containing inorganic nanoparticles in reflectance mode. (A) COM 1, (B) COM 2, (C) COM 3, (D) COM 4, (E) COM 5, (F) COM 6, and (G) ZnO nanoparticle standard. The microscope was equipped with a 561 nm HeNe laser and a 63 × objective (NA1.4). Scale bars represent 5 μm.**

presented extremely weak peaks for grain size calculations at 0.32% and 0.8% but sufficient intensities to enable particle size determination at 1.6% (24 nm). Similarly, rutile  $\text{TiO}_2$  exhibited weak signals that precluded sizing below 1.2%. In addition, the ZnO control sample showed peaks that enabled grain size

estimates above 1% (26 nm). Therefore, the limits of detection for anatase  $\text{TiO}_2$ , rutile  $\text{TiO}_2$ , and ZnO NPs were 1.6%, 1.2%, and 1%, respectively. Although the rutile  $\text{TiO}_2$  content of COM 4 (1.4%) was higher than its detection limit, the grain size in this sunscreen was underestimated, indicating that the organic

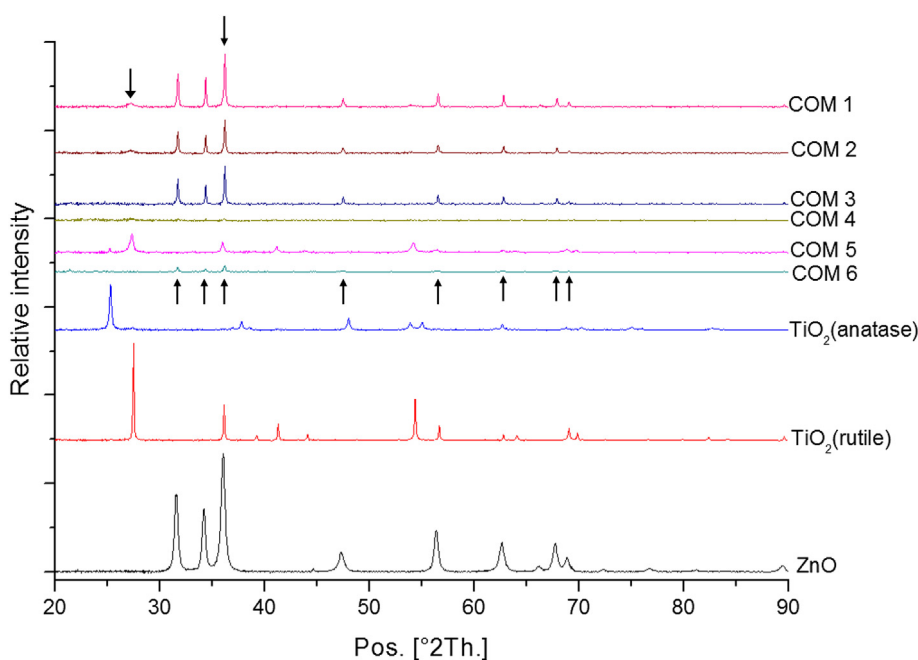


**Fig. 4 – X-ray diffraction patterns of commercial sunscreens COM 1–6 compared with anatase  $\text{TiO}_2$ , rutile  $\text{TiO}_2$ , and ZnO. Downward arrows indicate the  $2\theta$  positions for reflections arising from the rutile phase of  $\text{TiO}_2$  and upward arrows indicate  $2\theta$  positions for reflections arising from the ZnO wurtzite structure.**

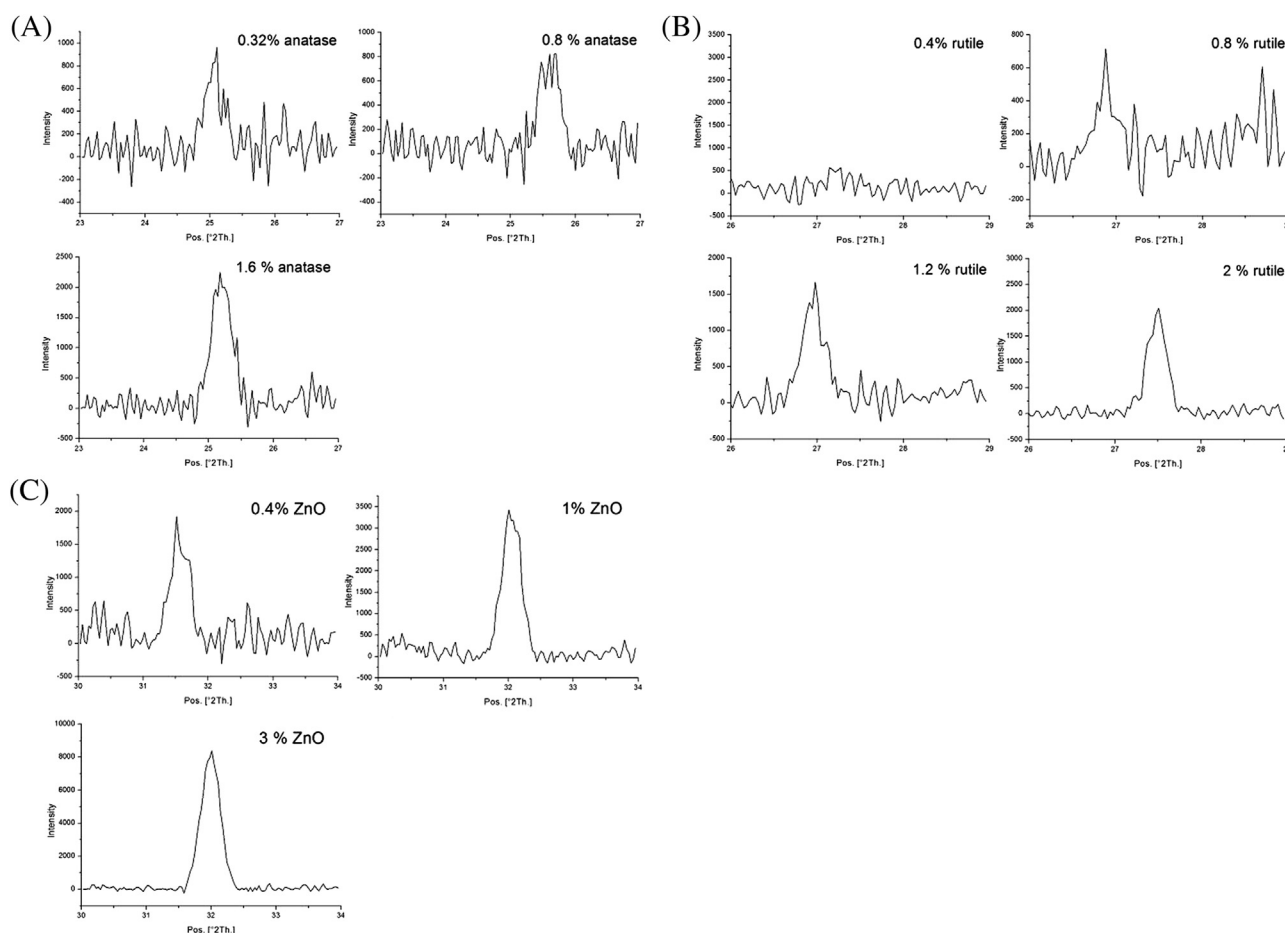


**Fig. 5** – X-ray diffraction patterns of anatase  $\text{TiO}_2$ , rutile  $\text{TiO}_2$ , and ZnO nanoparticle controls at different concentrations. (A) Diffraction patterns of anatase  $\text{TiO}_2$  controls. (B) Diffraction patterns of rutile  $\text{TiO}_2$  controls. (C) Diffraction patterns of ZnO controls.

matrix may interfere with size measurements. Therefore, XRD is suitable for crystal structure and mean particle size elucidation in unmodified sunscreens.

### 3.4. TEM analysis

Particle size, shape, and composition of commercial sunscreens were investigated by combining TEM with EDS. Samples needed dilution before TEM/EDS imaging. Electron micrographs of the samples clearly showed the NPs because the resolution was not affected by the rest of formulation (Fig. 6). Differences in particle shape were detected between samples. In particular, needle-shaped particles were found in COM 1, 2, and 4, while both needle shaped and spherical particles were observed in COM 5. Compositional analysis of inorganic residues by EDS demonstrated the presence of Si or Al signal closely match inorganic filter's signal in most samples. Reports have noted that  $\text{TiO}_2$  NP surfaces have been modified by silicon dioxide and aluminum oxide to reduce photoreactivity and minimize the formation of reactive oxygen species [14]. Scanning electron microscopy (SEM) was coupled with EDS to analyze the commercial sunscreens. The samples needed dilution before SEM/EDS imaging but the

charging of the surrounding organic matrix appeared to reduce the resolution (data not shown). Due to its high resolution, this suggests that TEM is more suitable than SEM for NP in these samples. In agreement with the International Cooperation on Cosmetic Regulation criteria [7], the six samples contained  $\text{TiO}_2$  and ZnO particles exhibiting at least one dimension smaller than 100 nm. COM 1 and COM 2 consisted of a mixture of  $\text{TiO}_2$  and ZnO NPs. XRD and TEM measurements provided consistent sizes and complementary nanomaterial characteristics (Table 2). Rutile  $\text{TiO}_2$  NPs exhibited needle-like shapes in COM 1, COM 2, and COM 4. Therefore, in COM 5, anatase and rutile  $\text{TiO}_2$  NPs were deduced to show spherical and needle-like shapes, respectively. These results demonstrate that XRD data were overlaid onto TEM data. Both XRD and TEM are suitable for size-related analysis in sunscreens.

## 4. Conclusion

Several analytical methods were applied to commercial sunscreens; however, some were not appropriate for the detection of NPs in these formulations. Specifically, AFM and LSCM

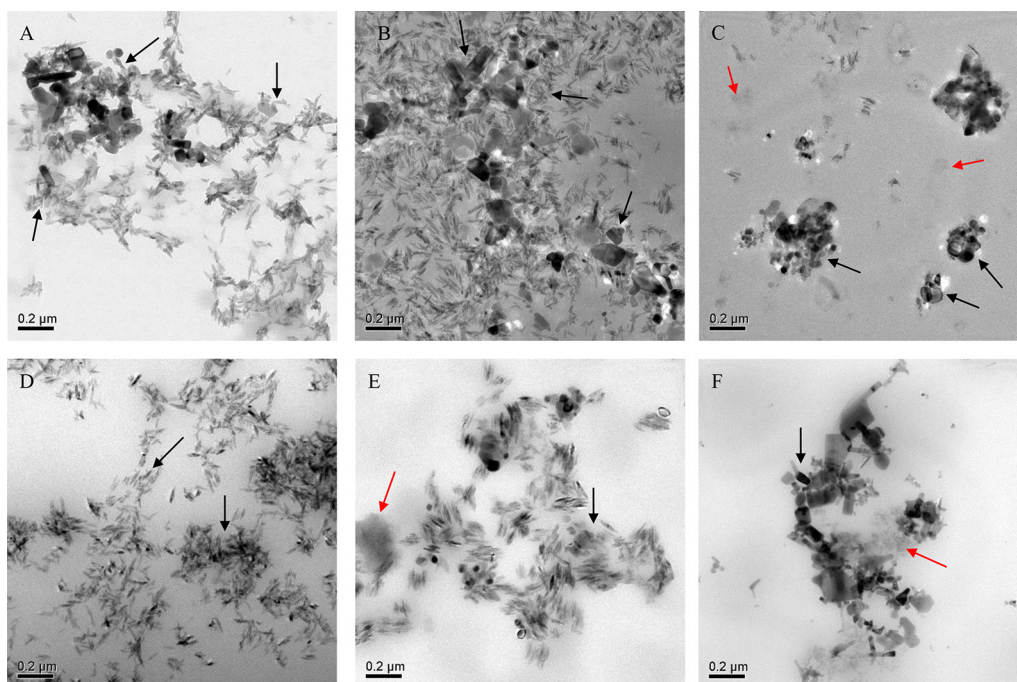


**Fig. 6 – Transmission electron microscopy of commercial sunscreens containing inorganic nanoparticles. (A) COM 1, (B) COM 2, (C) COM 3, (D) COM 4, (E) COM 5, and (F) COM 6. Images were acquired at a beam intensity of 200 kV and a magnification of 10,000–20,000 $\times$ . Black and red arrows indicated metal oxide NPs and the formulation matrix, respectively.**

**Table 2 – X-ray diffraction (XRD) and transmission electron microscopy (TEM) analytical results of commercial sunscreen samples and standards.**

| Product No.                  | XRD              |          |                | TEM                              |                |                            |
|------------------------------|------------------|----------|----------------|----------------------------------|----------------|----------------------------|
|                              | Particle         | Phase    | PPS (estimate) | Particle size (nm)               | Particle shape | Elements detected by EDS   |
| COM 1                        | TiO <sub>2</sub> | Rutile   | 15 nm          | 30–85 (length)<br>10–20 (width)  | Needle shaped  | Ti, Zn, C, O, Al, Si, (Cu) |
|                              | ZnO              | Wurtzite | 56 nm          | 50–110 (length)<br>25–90 (width) | various        |                            |
| COM 2                        | TiO <sub>2</sub> | Rutile   | 12 nm          | 45–85 (length)<br>10–15 (width)  | Needle shaped  | Ti, Zn, C, O, Al, Si, (Cu) |
|                              | ZnO              | Wurtzite | 59 nm          | 35–245 (length)<br>20–65 (width) | various        |                            |
| COM 3                        | ZnO              | Wurtzite | 64 nm          | 20–290 (length)<br>20–85 (width) | various        | Zn, C, O, Al, Si, (Cu)     |
| COM 4                        | TiO <sub>2</sub> | Rutile   | ? <sup>a</sup> | 45–95 (length)<br>10–20 (width)  | Needle shaped  | Ti, C, O, Al, Si, (Cu)     |
| COM 5                        | TiO <sub>2</sub> | Anatase  | 93 nm          | 25–100 (length)<br>20–80 (width) | Spherical      | Ti, C, O, Al, Si, (Cu)     |
|                              |                  | Rutile   | 33 nm          | 60–95 (length)<br>10–15 (width)  | Needle shaped  |                            |
| COM 6                        | ZnO              | Wurtzite | 47 nm          | 20–285 (length)<br>15–85 (width) | various        | Zn, C, O, Si, (Cu)         |
| TiO <sub>2</sub> NP standard | TiO <sub>2</sub> | Anatase  | 23 nm          | 4–48 (length)                    | various        | Ti, C, O, (Cu)             |
|                              |                  | Rutile   | 31 nm          | 3–40 (width)                     |                |                            |
| ZnO NP standard              |                  | Wurtzite | 29 nm          | 8–47 (length)<br>8–47 (width)    | Spherical      | Zn, C, O, (Cu)             |

EDS = energy-dispersive X-ray spectroscopy; PPS = primary particle size.

<sup>a</sup> Unavailable information.

were unsuitable for characterizing inorganic oxides in unmodified and complex commercial sunscreens. By contrast, XRD and TEM identified TiO<sub>2</sub> and ZnO NP sizes in these samples and gave complementary information about characterizing NPs. XRD was able to show crystal structure and mean particle size in unmodified sunscreens; TEM was able to show the particle size, shape, and composition of commercial sunscreens. Although both methods were constant in sizing results, some limits were presented. XRD was not an imaging method able to observe the NPs in the formulations and cannot size above ca. 200 nm. TEM can resolve the NPs in the matrix, but samples needed dilution before the observation. The dilution condition may alter the NPs and cannot analyze the aggregation/agglomeration state in the final products. Despite the limited methods, new techniques are being developed constantly. We are looking for new analytical methods to determine the aggregation/agglomeration state, and expect that these analytical methods may be exploited by competent health authorities and cosmetic manufacturers.

### Conflicts of interest

All authors declare no conflicts of interest.

### REFERENCES

- [1] Wiesenthal A, Hunter L, Wang S, Wickliffe J, Wilkerson M. Nanoparticles: small and mighty. *Int J Dermatol* 2011;50:247–54.
- [2] Lorenz C, Tiede K, Tear S, Boxall A, Von Goetz N, Hungerbühler K. Imaging and characterization of engineered nanoparticles in sunscreens by electron microscopy, under wet and dry conditions. *Int J Occup Environ Health* 2010;16:406–8.
- [3] Smijs TG, Pavel S. Titanium dioxide and zinc oxide nanoparticles in sunscreens: focus on their safety and effectiveness. *Nanotechnol Sci Appl* 2011;4:95–112.
- [4] Zvyagin AV, Zhao X, Gierden A, Sanchez W, Ross JA, Roberts MS. Imaging of zinc oxide nanoparticle penetration in human skin *in vitro* and *in vivo*. *J Biomed Opt* 2008;13:064031–8.
- [5] Tilman B, Tilo R, Teresa P, Philippe M, Jan P, Árpád ZK, Jerzy S, Wojciech D, Zbigniew S, Janusz L, Małgorzata L, Janos H, Tamás B, Michael S, Luc VV, Pieter VR, Jean-Etienne SB. NanoDerm: quality of skin as a barrier to ultra-fine particles. 2007. Available at: [http://www.uni-leipzig.de/~nanoderm/Downloads/Nanoderm\\_Final\\_Report.pdf](http://www.uni-leipzig.de/~nanoderm/Downloads/Nanoderm_Final_Report.pdf).
- [6] Wu J, Liu W, Xue C, Zhou S, Lan F, Bi L, Xu H, Yang X, Zeng FD. Toxicity and penetration of TiO<sub>2</sub> nanoparticles in hairless mice and porcine skin after subchronic dermal exposure. *Toxicol Lett* 2009;191:1–8.
- [7] International Cooperation on Cosmetic Regulation. Report of the ICCR Joint Ad Hoc Working Group on Nanotechnology in Cosmetic Products: Criteria and Methods of Detection - ICCR-4. 2010.
- [8] ISO/TR 13014:2012 Nanotechnologies—guidance on physico-chemical characterization of engineered nanoscale materials for toxicologic assessment. Geneva, Switzerland: International Organization of Standards; 2012.
- [9] Food and Drug Administration. Guidance for industry safety of nanomaterials in cosmetic products. 2014. Available at: <http://www.fda.gov/downloads/Cosmetics/GuidanceRegulation/GuidanceDocuments/UCM300932.pdf>.
- [10] Zhang Y, Chen Y, Westerhoff P, Hristovski K, Crittenden JC. Stability of commercial metal oxide nanoparticles in water. *Water Res* 2008;42:2204–12.
- [11] Warheit DB, Webb TR, Reed KL, Frerichs S, Sayes CM. Pulmonary toxicity study in rats with three forms of ultrafine-TiO<sub>2</sub> particles: differential responses related to surface properties. *Toxicology* 2007;230:90–104.
- [12] Tyner KM, Wokovich AM, Doub WH, Buhse LF, Sung LP, Watson SS, Sadrieh N. Comparing methods for detecting and characterizing metal oxide nanoparticles in unmodified commercial sunscreens. *Nanomedicine* 2009;4:145–59.
- [13] Scientific Committee on Consumer Safety. Guidance on the safety assessment of nanomaterials in cosmetics. 2012. Available at: [http://ec.europa.eu/health/scientific\\_committees/consumer\\_safety/docs/sccs\\_s\\_005.pdf](http://ec.europa.eu/health/scientific_committees/consumer_safety/docs/sccs_s_005.pdf).
- [14] Lewicka ZA, Benedetto AF, Benoit DN, Yu WW, Fortner JD, Colvin VL. The structure, composition, and dimensions of TiO<sub>2</sub> and ZnO nanomaterials in commercial sunscreens. *J Nanopart Res* 2011;3:3607–17.